


Development of a Bioartificial Vascular Pancreas

Journal of Tissue Engineering
Volume 12: 1–18
© The Author(s) 2021
Article reuse guidelines:
sagepub.com/journals-permissions
DOI: 10.1177/20417314211027714
journals.sagepub.com/home/tej



Edward X Han¹ , Juan Wang^{2,3}, Mehmet Kural^{2,3},
Bo Jiang^{4,5}, Katherine L Leiby¹, Nazar Chowdhury⁶,
George Tellides^{2,4,7}, Richard G Kibbey^{8,9},
Jeffrey H Lawson^{10,11} and Laura E Niklason^{1,2,3,11}

Abstract

Transplantation of pancreatic islets has been shown to be effective, in some patients, for the long-term treatment of type I diabetes. However, transplantation of islets into either the portal vein or the subcutaneous space can be limited by insufficient oxygen transfer, leading to islet loss. Furthermore, oxygen diffusion limitations can be magnified when islet numbers are increased dramatically, as in translating from rodent studies to human-scale treatments. To address these limitations, an islet transplantation approach using an acellular vascular graft as a vascular scaffold has been developed, termed the BioVascular Pancreas (BVP). To create the BVP, islets are seeded as an outer coating on the surface of an acellular vascular graft, using fibrin as a hydrogel carrier. The BVP can then be anastomosed as an arterial (or arteriovenous) graft, which allows fully oxygenated arterial blood with a pO_2 of roughly 100 mmHg to flow through the graft lumen and thereby supply oxygen to the islets. In silico simulations and in vitro bioreactor experiments show that the BVP design provides adequate survivability for islets and helps avoid islet hypoxia. When implanted as end-to-end abdominal aorta grafts in nude rats, BVPs were able to restore near-normoglycemia durably for 90 days and developed robust microvascular infiltration from the host. Furthermore, pilot implantations in pigs were performed, which demonstrated the scalability of the technology. Given the potential benefits provided by the BVP, this tissue design may eventually serve as a solution for transplantation of pancreatic islets to treat or cure type I diabetes.

Keywords

Tissue engineering, Islet transplantation, Type I diabetes, Vascular graft, Cell-based therapeutics

Date received: 10 April 2021; accepted: 8 June 2021

¹Department of Biomedical Engineering, Yale School of Engineering and Applied Science, New Haven, CT, USA

²Vascular Biology and Therapeutics Program, Yale School of Medicine, New Haven, CT, USA

³Department of Anesthesiology, Yale School of Medicine, New Haven, CT, USA

⁴Department of Surgery, Yale School of Medicine, New Haven, CT, USA

⁵Department of Vascular Surgery, The First Hospital of China Medical University, Shenyang, China

⁶Molecular, Cellular, and Developmental Biology, Yale University, New Haven, CT, USA

⁷Veterans Affairs Connecticut Healthcare System, West Haven, CT, USA

⁸Department of Internal Medicine (Endocrinology), Yale University, New Haven, CT, USA

⁹Department of Cellular & Molecular Physiology, Yale School of Medicine, New Haven, CT, USA

¹⁰Department of Surgery, Duke University, Durham, NC, USA

¹¹Humacyte Inc., Durham, NC, USA

Corresponding author:

Laura E Niklason, Nicholas M. Greene Professor and Vice Chair, Anesthesiology and Biomedical Engineering, Vascular Biology and Therapeutics, Yale School of Engineering and Applied Science, PO Box 208089, New Haven, CT 06520-8089, USA.

Email: laura.niklason@yale.edu



Introduction

Type 1 diabetes results from the autoimmune destruction of pancreatic islets and is a growing and chronic health problem throughout the world.^{1,2} Monitoring of blood sugar levels, and recurrent intervention with exogenous insulin, allow many patients to lead relatively normal lives. However, diabetes still causes numerous short-term complications such as hyper- and hypo-glycemic episodes, and long-term complications such as cardiovascular disease and diabetic nephropathy.^{3,4} Transplantation of pancreatic islet cells can restore endocrine control of blood sugar levels and provides patients with improved glycemic control to avoid the debilitating side effects of diabetes.⁵ Unfortunately, current strategies for clinical islet transplantation suffer from issues such as islet inflammation from direct blood contact, hypoxia, and inadequate nutrient transfer, leading to islet cell death due to limitations in nutrient transfer/oxygenation, and transplant failure.^{6–10}

Native islets require high levels of oxygen to survive: islets utilize 5%–20% of the oxygen provided to the pancreas, despite making up only 1%–2% of pancreatic mass.^{11,12} Given the high metabolic demands of islets, it is evident that islet transplant strategies require attention to oxygenation to achieve sufficient islet survival. Many islet therapies such as implantation of islets into the intra-abdominal cavity or into the sub-cutaneous space, transplant islets into environments where the local pO_2 is typically only ~40 mmHg.^{13–16} This can lead to islet death during the early post-transplant period before revascularization of transplanted islets by the host. Islets transplanted into the portal vein of the liver using the Edmonton Protocol, where the pO_2 of the portal blood is often near 40 mmHg, face local hypoxia as well as acute thrombosis around the islets.^{5,17,18} Up to 50% of transplanted islets are immediately lost upon transplantation due to the instant blood mediated inflammatory reaction caused by a combination of acute thrombosis and leukocyte infiltration.^{19,20} The islets then face hypoxia, due to low oxygen levels in portal vein blood.²¹ This hypoxic environment can lead to eventual graft failure, if capillary ingrowth does not occur quickly enough to support islet survival.⁸ As a result, multiple injections of islets are required, and the success rate of the Edmonton Protocol after 5 years is only 25%–50%.^{22–26}

To protect transplanted islets from immune recognition, microencapsulation is commonly used,^{27,28} wherein islet-embedded microcapsules are implanted either subcutaneously or intraperitoneally.^{29–32} While each individual microcapsule is able to support enough diffusion for islet survival, combining tens to hundreds of thousands of microcapsules in the subcutaneous or intraperitoneal space can lead to clumping and local depletion of oxygen and nutrients.³³ Low oxygen levels in islet encapsulation techniques suggest that focusing on improving islet oxygen delivery and vascular integration may be a road toward better islet transplantation results.

Higher local oxygen levels increase the likelihood that islets will survive the early, avascular post-transplant period long enough to allow for revascularization. To facilitate oxygen delivery, some approaches utilize implantable devices with external oxygen ports or oxygen generating materials. However, these techniques have not yet demonstrated sustained islet viability in islet transplant recipients.^{34,35} For vascular integration, directly connecting an islet transplant device with the arterial system of the host, to create a vascularized islet delivery device would allow islets to be in close proximity to constantly replenishing oxygen in the arterial bloodstream. Initial attempts to create such a vascular delivery device began to take shape in the 1990s with work by Monaco and Sullivan.^{36,37} However, these perfused, vascular artificial pancreata were not successful *in vivo*, in part because of high rates of thrombosis of the synthetic materials used for the vascular conduit.³⁸ Progressions in vascular engineering, specifically in decellularized vessel engineering, have yielded vascular grafts with improved biocompatibility that allow us to re-examine this methodology for islet transplantation.

Vascular grafts made from acellular biological extracellular matrices do not utilize oxygen from the bloodstream and have a lower rate of thrombosis than grafts made from artificial materials,^{39–47} and oxygen can diffuse from the bloodstream through the wall of the acellular matrices, thereby providing a means to oxygenate cells or tissues that are applied on the outer surface of the vascular conduits. An acellular vascular graft that is 40 cm in length and 6 mm in diameter – similar to that used as an arteriovenous graft in the arm for dialysis access – could accommodate roughly 800,000 islets on its outer surface, which is approximately the normal total islet complement of an adult human.^{48,49} Therefore, clinically-relevant dimensions of acellular vessels could accommodate islet numbers that may be suitable for therapy in type 1 diabetes.⁵⁰

It is this general approach for islet delivery that we sought to test in this report. We evaluated the delivery of pancreatic islets using an acellular vessel as a scaffold, to deliver islets in close proximity to, but not within, the arterial blood circulation. We hypothesized that seeding islets on the outer surface of an acellular vessel would allow for improved islet survival and functionality compared to transplantation of islets without connection to the arterial circulation. We term this approach the “Biovascular Pancreas,” or BVP (Figure 1). To determine the ultimate utility of the BVP concept and to optimize parameters of its design, we performed *in silico* modeling (computer simulations) using finite element analysis. These results were validated by *in vitro* bioreactor studies designed to mimic oxygen levels in implanted BVP constructs. Finally, to demonstrate the therapeutic effect of the BVP, we performed *in vivo* implantations into nude rats and piloted implantation studies into adult swine.

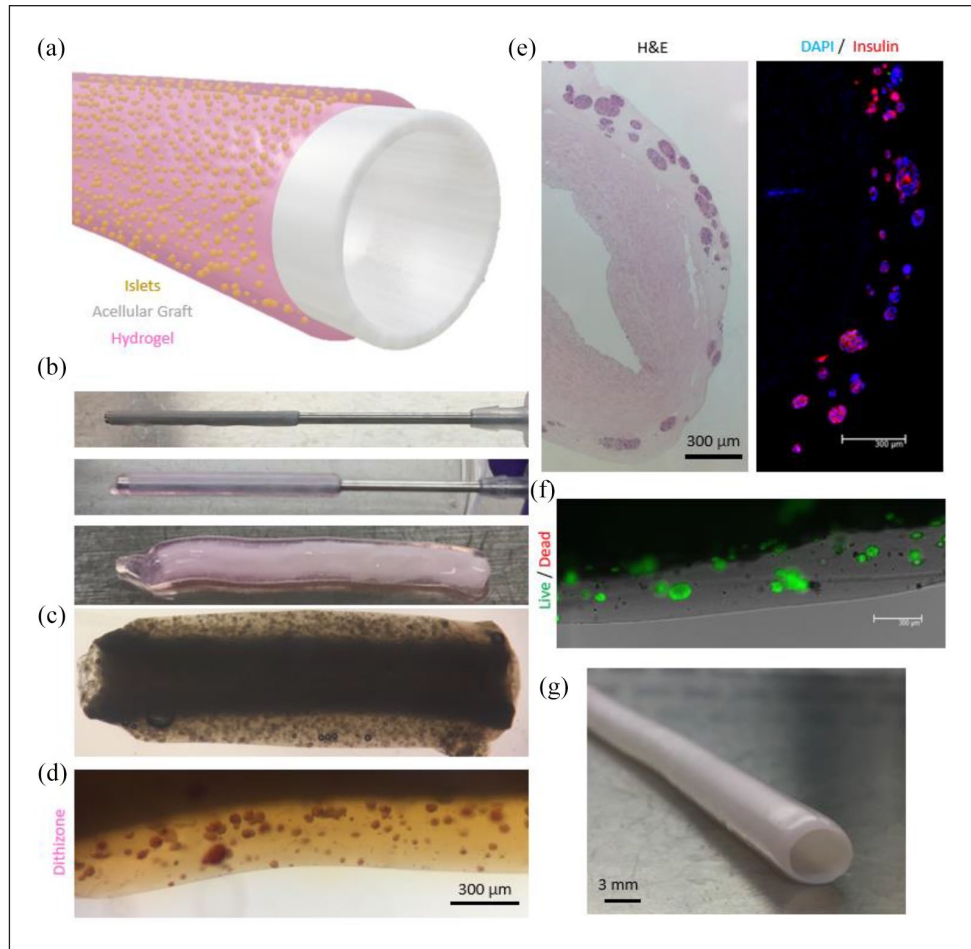


Figure 1. BioVascular Pancreas (BVP) tissue design and fabrication: (a) schematic of BVP tissue containing an acellular graft and pancreatic islets coated on the outer surface using a hydrogel carrier, (b) fabrication process of the rat-sized BVP using a molding technique, (c) rat-sized BVP shown under light microscopy (d) and shown with dithizone staining to indicate islet purity, (e) circular cross-section of the BVP stained using H&E, (f) fluorescent microscopy image of BVP coating with live/dead stain demonstrating islet survival after BVP creation, and (g) pig/human sized BVP.

Results

Device creation

The BVP consists of an acellular vessel wall, with islets coated on the outer surface using a fibrin hydrogel (Figure 1(a)). Fibrin was selected as the hydrogel of choice due to the fact that it has shown success in islet transplantation studies, facilitates microvessel ingrowth, and has an easy-to-use crosslinking mechanism achieved by combining fibrinogen with thrombin.^{51–55}

Rat-sized BVPs were created using rat pancreatic islets coated around decellularized human umbilical arteries (DHUA) that were 1 mm in diameter and 1–1.5 cm in length, with a wall thickness of 300–500 μm .^{56,57} Pancreatic islets were isolated from adult rat pancreata using a series of enzymatic digestion steps, and then were coated onto the outer surface of DHUA by combining islets, fibrinogen, and thrombin together into a mold containing the DHUA (Figure 1(b)). Rat BVPs were seeded with ~1500

islet equivalents (IEQs), resulting in a density of roughly 15 IEQs/ μL in the coating layer (Figure 1(c)). In comparison, a previous study performed seeded islets in fibrin at a density of roughly 12.5 IEQs/ μL .⁵²

Dithizone staining (Figure 1(d)) of circular cross sections of BVPs demonstrated that islets were fairly evenly coated on the DHUA, and the coating thickness was approximately 400 μm (Figure 1(e)). Live/dead staining using fluorescein diacetate (FDA) and propidium iodide (PI) showed that islets survived the coating procedure (Figure 1(f)).

Porcine BVPs were created using a similar molding technique, but around a larger human acellular engineered vessel that had been cultured in vitro from human vascular smooth muscle cells and then decellularized (Figure 1(g)). Human acellular vessels were of suitable dimensions for arterio-venous grafting,⁴⁷ and were 6 mm diameter and 40 cm in length, with a wall thickness of approximately 440 microns (gift from Humacyte Inc.). Porcine islets were isolated from

adult Yorkshire pigs using a standard collagenase digestion / histopaque gradient protocol. Similar to rat BVP creation, porcine BVPs were created using a molding procedure with the acellular graft, islets, fibrinogen, and thrombin.

Modeling of BVPs of varying dimensions

In silico modeling in COMSOL Multiphysics was used to investigate and predict diffusion properties of oxygen in the BVP, as well as to predict oxygen levels that would attend delivery of an equivalent number of islets as a single spherical bolus or injection. Oxygen consumption rates were simulated using Michaelis-Menten equations, including known parameters for islet oxygen consumption (described in detail in Methods section).^{58–60} The modeled geometry elements included a decellularized vessel of specified diameter and wall thickness, a hydrogel coating layer of known thickness that was seeded with a stochastic distribution of pancreatic islets, a lumen of the decellularized vessel, and an interstitial space outside the vessel coating (Figure 2(a) and (b)). Specific dimensions of the model are shown in Figure 2(a) and (b).

To simulate the islets themselves, islet diameter is an essential parameter.⁷ Mammalian islet diameters can range from <50 to 500 μm , described by a positive skew Weibull distribution with a with most islets ranging from 50 to 150 μm in diameter.⁶¹ Islets were stochastically assigned diameters based on a Weibull distribution (Supplemental Figure 1), and were assigned randomly distributed positions throughout the hydrogel coating layer.^{58,62}

To simulate in vivo conditions, the oxygen level of the BVP lumen was set to 100 mmHg to mimic the pO_2 of arterial blood within an arterial or arteriovenous graft, while the interstitial space surrounding the BVP was set to 40 mmHg. We compared predicted islet viability and oxygen diffusion levels in the BVP to those which might be seen in a spherical injection of a similar number of islets into the subcutaneous or intraperitoneal space, using matched islet numbers and density within the hydrogel carrier (Supplemental Table 1).³³ The spherical volume control was chosen as a simplified representation of transplanted microspheres which tend to clump after transplantation and experience pericapsular fibrotic overgrowth.³³

For characterization of oxygen levels, surface integration was performed to determine the area and volume of islet cells having oxygen levels below the hypoxia threshold, 0.1 μM (0.07 mmHg) O_2 .⁵⁹ (While mitochondrial performance and cellular functionality suffer below ~ 2 mmHg, anaerobic respiration provides leeway for cell survival and definitive hypoxic cell death is commonly quoted to occur at ~ 0.1 mmHg^{61,63–66}). The area of the BVP implant having O_2 levels below 0.1 μM O_2 was then compared to the total islet area to determine the fractional area of islet survival. Visually, hypoxic areas below the 0.1 μM O_2 threshold are shown in white (Figure 2(c) and (d))

(Supplemental Figures 2–4) and were quantified using surface integration (Figure 2(e) and (f)). Since simulations were performed with randomly distributed islets and islet diameters following a Weibull distribution, multiple simulations were performed per condition to account for variability between simulation runs. To verify that simulation results correlated with in vitro results, a simple experiment was performed where islets were seeded in fibrin in a 96 well plate, an equivalent simulation was then created, and results showed that hypoxic areas below 0.1 μM O_2 coincided well with areas that stained positive for propidium iodide which indicates cell death (Supplemental Figure 2). In addition, since islet functionality and insulin secretion are negatively impacted below 3 μM O_2 (2 mmHg) O_2 , simulations with a 3 μM O_2 threshold were also performed to determine the percent of islet mass functionally capable of sustained insulin secretion (Figure 2(e) and (f)).

Simulation results revealed that increasing islet seeding number up to 5000 islets (density = 180,000 islets/mL) for rat BVPs and 1,000,000 islets (density = 280,000 islets/mL) for human BVPs resulted in relatively minimal losses in predicted survival. (Supplemental Figures 3 and 4 show model results in more detail). Given that it is estimated roughly 1500 rat islets are required to cure diabetes in rats, and 500,000 human IEQs are sufficient to cure diabetes in humans using the Edmonton protocol that has limited islet viability,⁵⁰ the simulations demonstrate that the BVP can theoretically support a sufficient number of islets for a therapeutic effect (Figure 2(e) and (f)).

In contrast, for a 1500 islet rat BVP, only 65% of islet mass is above the insulin functionality threshold of 3 μM oxygen. For a 500,000 islet human BVP, 50% of islet mass is above 3 μM oxygen concentration. Assuming that the majority of islets are able to survive the initial environment of the BVP however, gradual microvascularization of the islets may increase the percentage of functional islets in the BVP over time, and thus improve BVP performance. To test this, simulations incorporating microvessels into the coating layer were performed. Microvessels 8 μm in diameter were scattered randomly into the coating layer using a simulation approach.^{67,68} These microvessels were assigned oxygen concentrations at 40 mmHg O_2 . Varying percent area coverages of microvessels were tested. In implanted fibrin tissues, microvascularization occurs with a percent area coverage ranging from 0.5% to 2% (Supplemental Figure 5).⁶⁹ Results demonstrated that if the BVP could achieve 0.5% microvessel coverage, the percent functional area for islets would increase to $\sim 100\%$ (Supplemental Figure 5). These simulations support the hypothesis that microvessel infiltration can be greatly beneficial to ensuring seeded islets eventually get enough oxygen to allow for their full insulin secreting capabilities.

Compared to the spherical volume controls, 1500 IEQs have a predicted survival <35% and insulin functionality <10%, while 500,000 IEQs have a predicted survival

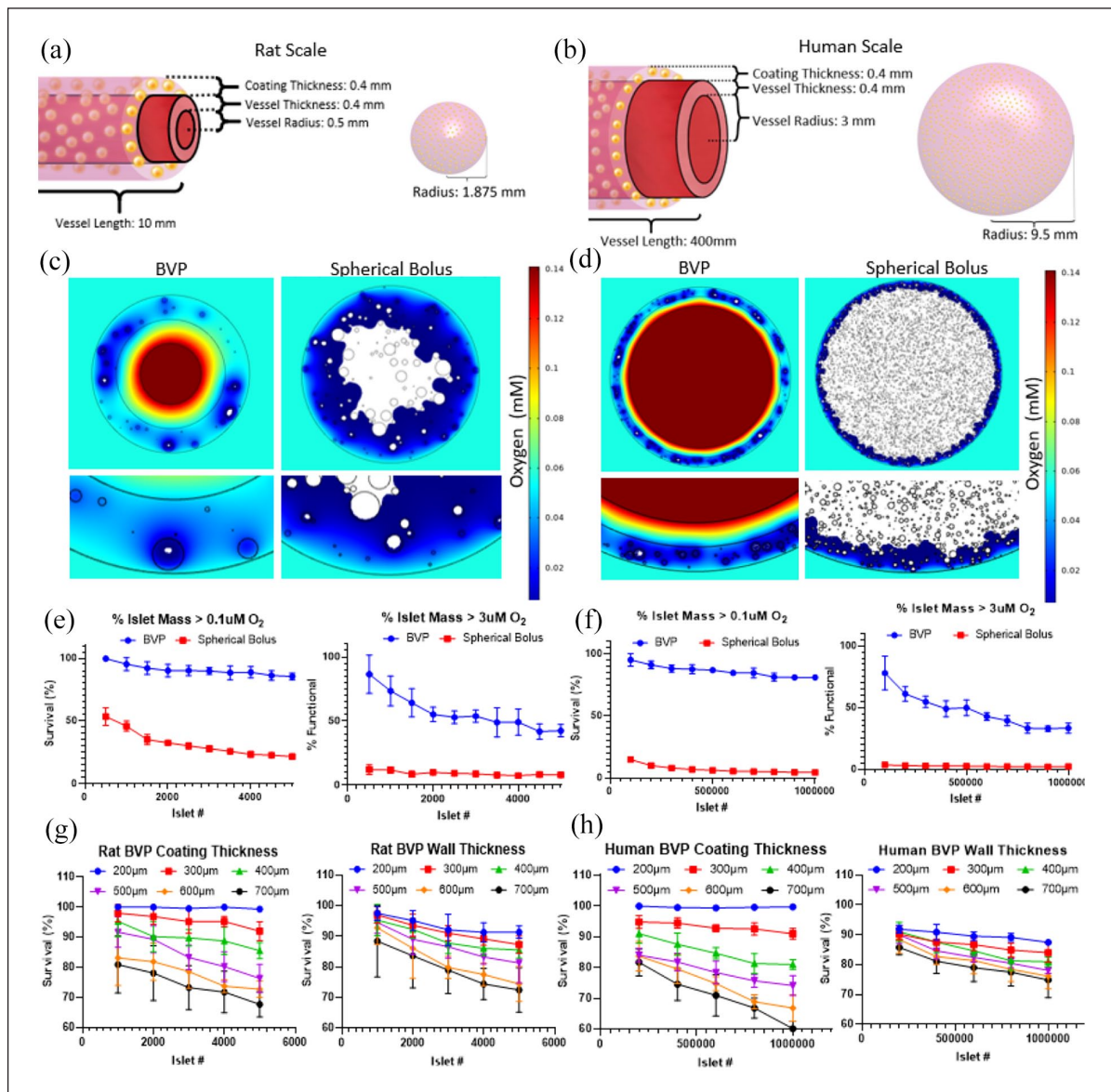


Figure 2. In silico characterization of oxygen concentrations and oxygen consumption by pancreatic islets in the BVP. Dimensions for Rat (a) and Human (b) sized BVPs and equivalent spherical volumes. (c) Oxygen concentration simulations performed using Michaelis-Menten equations of BVPs and spherical volumes seeded with islets for rat and (d) human ($n = 5$ stochastic simulations per parameter). (c) Shows a simulation performed using the dimensions shown in (a) with a total of 1500 IEQs while (d) shows a simulation performed using the dimensions shown in (b) with a total of 500,000 IEQs. Areas with oxygen concentration below the hypoxic threshold of $0.1 \mu\text{M}$ are shown in white. (e) Surface integration below the hypoxic threshold of $0.1 \mu\text{M}$ (left) and below the physiological functionality threshold of $3 \mu\text{M}$ (right) for varying islet numbers at rat and (f) human scales. (g) and (h) Stochastic simulations demonstrating the effect of varying coating thickness or wall thickness on islet survival rates ($n = 5$ stochastic simulations per parameter).

$<10\%$ and insulin functionality $<5\%$. Any configuration where large numbers of islets are transplanted in confined volumes within a low- O_2 environment (i.e. subcutaneous space, intraperitoneal space) would be characterized by similar outcomes of low oxygenation for therapeutic doses of islets.

Parameters such as coating thickness and vessel wall thickness were varied to determine the effect on local

oxygen concentrations. Areas below the hypoxic threshold of $0.1 \mu\text{M}$ O_2 were then quantified to predict islet survival (Figure 2(g)). When varying wall thickness, survival rates for a 5000 IEQ rat BVP with a coating thickness of $400 \mu\text{m}$ were estimated to be 95%, 85%, and 75% with wall thicknesses of 200, 400, and $700 \mu\text{m}$, respectively. Analogous relationships between survival and coating/wall thickness could also be seen for human sized BVPs (Figure 2(h)).

The simulations also show that coating thickness has a greater effect on predicted islet cell survival than does vessel wall thickness.

In vitro culture and bioreactor studies

Rat-sized BVPs were made from decellularized human umbilical arteries, fibrin, and 1500 rat IEQs. 1500 IEQs were used since modeling results demonstrated adequate survival for 1500 IEQs in the rat-scale results. In addition, multiple studies in the literature have utilized around 1500 IEQs for rat islet transplantation.^{70,71} Fibrin was used at 10 mg/mL since it provided favorable islet survival and acceptable mechanical properties (Supplemental Figure 6). DHUAs, approximately 1–2 mm in diameter, were selected instead of decellularized rat vessels since large rat vessels such as the abdominal aorta and thoracic aorta all contain multiple branching arterioles that are difficult to ligate. Implantation of a BVP made using these vessels would be difficult due to blood leakage from these numerous side branches. Furthermore, branchless DHUAs have been implanted successfully as interposition aortic grafts in rats. For static culture glucose tolerance tests, insulin release was assessed by incubating freshly-constructed BVPs held at 160 mmHg pO₂ in low-glucose media (<20 mg/dL) for 60 min, followed by normal glucose (180 mg/dL) for 120 min. As expected, insulin release was low when the BVP was incubated in low-glucose media, but rapidly increased at 180 mg/dL glucose, showing responsiveness of the islets and BVP construct (Figure 3(a)). However, BVPs that were first statically incubated overnight at 40 mmHg O₂, with no luminal flow of culture medium, displayed decreased insulin secretion compared to the BVPs that were tested immediately after creation (Figure 3(a)). This shows the decrement in islet function after only 24 h of non-perfusion in conditions mimicking the interstitial space.

To evaluate insulin release under conditions of intraluminal flow mimicking arterial or arteriovenous implantation, bioreactors were assembled with a circulating flow path through the lumen of the BVP at 100 mmHg pO₂, and medium surrounding the BVP maintained at 40 mmHg pO₂ (Figure 3(b)). Flow rate in the bioreactor was set to 10 mL/min to mimic abdominal aortic flow in a rat.⁷² Glucose tolerance testing demonstrated that BVPs in flowing bioreactors trended higher in insulin release at later time points, perhaps due to the convective properties associated with the bioreactor setup, including increased oxygen delivery and removal of secreted insulin. Quantitatively, a rat-sized BVP in the flow bioreactor could secrete approximately 25 µg of insulin in 2 h. Given that a rat requires approximately 3–4 IU (102–136 µg) of insulin per day to maintain normoglycemia, the bioreactor studies showed that the rat-sized BVP should secrete enough sufficient insulin to meet rat daily requirements.⁷³

To quantify the impact of the BVP design on islet viability and function, bioreactor flow conditions were compared to static incubation of the rat-sized BVPs at either 160 mmHg pO₂ (hyperoxic) or 40 mmHg pO₂ (interstitial

oxygen levels). In silico simulations predicted that static incubation at 160 mmHg should result in some hypoxia (>50% survival) while static incubation at 40 mmHg should create a strongly hypoxic environment (<30% survival), and in vivo/bioreactor conditions should result in minimal hypoxia (>90% survival) (Figure 3(c) and (d)). Survival of islets in the bioreactor for up to 2 days was assessed using FDA/PI live/dead staining (Figure 3(c) and (d)). Islet survival rate for BVPs in the bioreactor was around 90%, and was considerably higher than for islets in BVPs that were incubated statically at 40 mmHg pO₂, which had a survival rate around 50%. These observations were corroborated by HIF1-α immunostaining, showing increased HIF1-α in nuclei in the static 40 mmHg pO₂ condition, indicative of functional cellular hypoxia (Figure 3(c)). In contrast, HIF1-α staining was not evident in the static 160 mmHg pO₂ condition, nor in the bioreactor culture condition.

In vivo rat studies

Nude rats were induced with diabetes using intraperitoneal injections of streptozotocin, and were considered diabetic when consecutive daily blood glucose measurements exceeded 400 mg/dL (Supplemental Figure 7). For context, normal blood glucose levels for nude rats are typically between 100 to 200 mg/dL.⁷⁴ Nude rats were selected as graft recipients to avoid confounding factors of immunosuppression which would be required to prevent rejection of the bovine fibrinogen and thrombin used to construct the coating layer of the BVP. Streptozotocin-induced nude rats each received a 1 cm BVP containing 1500 (1470 ± 160) IEQs as an end-to-end interposition graft in the rat abdominal aorta (*n* = 5, Figure 4(a)) (Supplemental Video 1). BVPs remained in situ for 90–100 days, and blood samples were taken intermittently to document blood glucose and insulin levels. As controls, identical BVP constructs were placed adjacent to the abdominal aorta within the abdominal cavity, but without anastomosing to the arterial circulation (*n* = 3). In this way, the BVP was placed into the recipient without any direct vascularization – these were the “no flow” implants.

BVPs were explanted by repeat laparotomy after the prescribed implantation time. At time of explantation, anastomosed BVPs had extensive microvascular infiltration, which may have been supported by islet secretion of angiogenic factors, as well as the fibrin hydrogel carrier (Figure 4(b)).

Rats that received an anastomosed BVP implant demonstrated a gradual decrease in blood glucose levels over the course of 1–2 months (Figure 4(c)). Rapid reversal of diabetes was not observed. This may be partially attributable to the fact that modeling results showed that oxygen availability in the BVP is sufficient for islet survival but is not sufficient for maximal insulin secretion. We speculate that as microvascularization occurs around the implanted islets, the islets have improved oxygen availability and

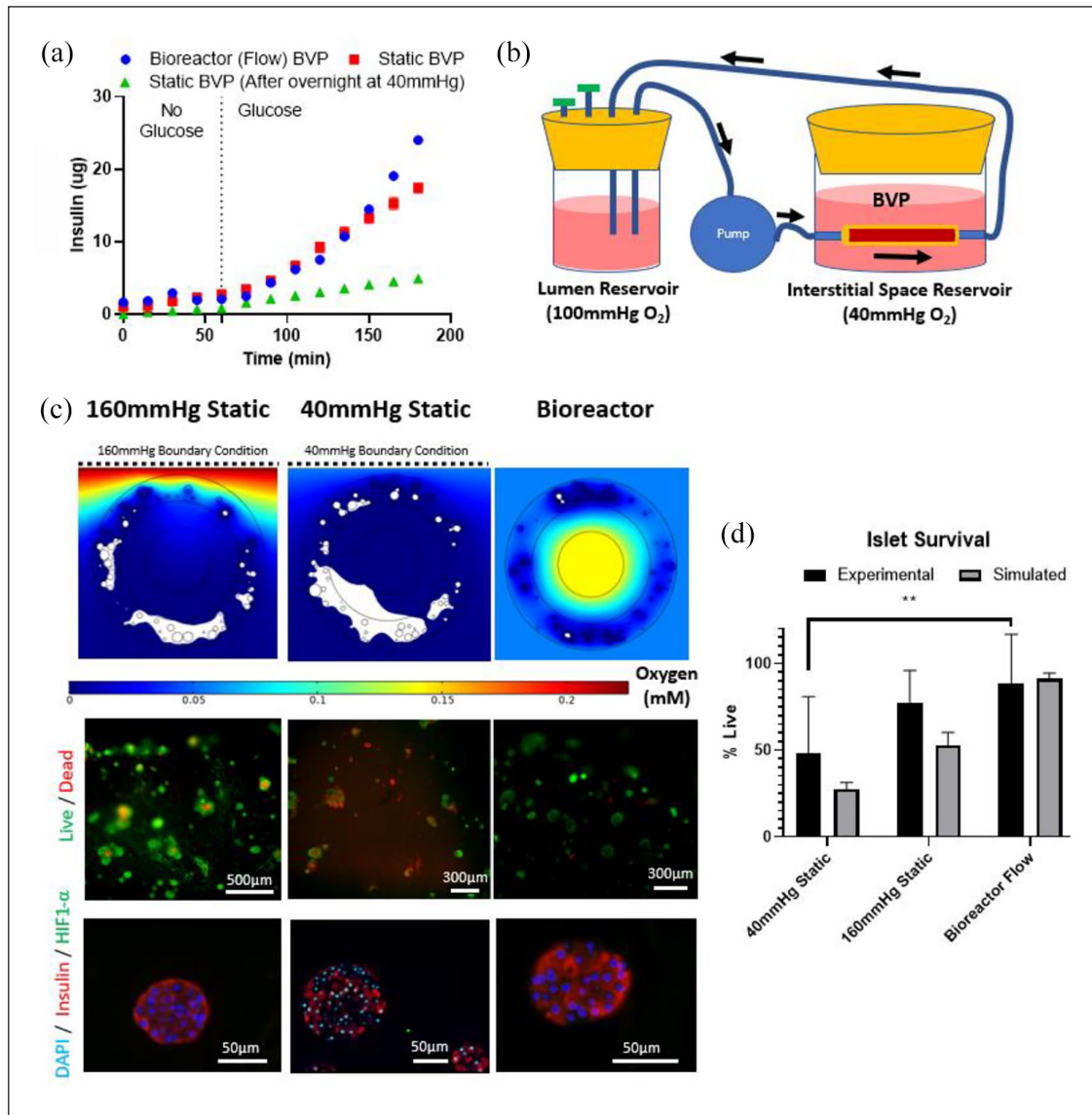


Figure 3. Insulin release and survival percentages in BVPs tested in vitro. (a) Glucose tolerance test performed on BVPs exposed to luminal flow or on static BVPs either immediately after creation, or after overnight incubation at 40 mmHg O₂. (b) Flow bioreactor setup for the BVP designed to mimic in vivo conditions. (c) Simulations (top), in vitro live/dead staining (middle) and HIF1- α staining (bottom) of BVPs statically incubated at 160 mmHg O₂, statically incubated at 40 mmHg O₂, or in the bioreactor setup shown in (b). (d) Quantification of survival percentages for simulations and in vitro live dead staining shown in (c). Statistical significance between experimental 40 mmHg Static and experimental bioreactor group determined using unpaired, two-tailed *t*-test (***p* = 0.0072) (*n* = 3).

functionality which then causes blood glucose levels to gradually decline over time. In contrast, rats that received “no flow” BVP implants maintained high blood glucose levels, averaging >400 mg/dL, throughout the entire experiment. Since “no flow” implants contained the same number of islets as BVPs implanted in the aorta, but lacked arterial blood flow through the lumen of the BVP, it is likely that the significant differences in blood glucose are attributable to islet survival in the setting of intra-arterial BVP implantation. Using two consecutive measurements below 250 mg/dL as a criterion for euglycemia,⁷⁰ all

intra-aortic BVPs restored euglycemia by day 80, while none of the “no flow” implants restored euglycemia (Figure 4(d)). Average blood plasma insulin levels were also statistically higher in anastomosed BVP rats as compared to no flow BVP rats (Figure 4(e)).

Islet graft removal is oftentimes performed before animal sacrifice to verify a return to hyperglycemia and confirm that diabetes reversal is a result of transplanted islets as opposed to recipient recovery from streptozotocin. Unfortunately, the difficulty of performing a second graft insertion after BVP removal from the rat

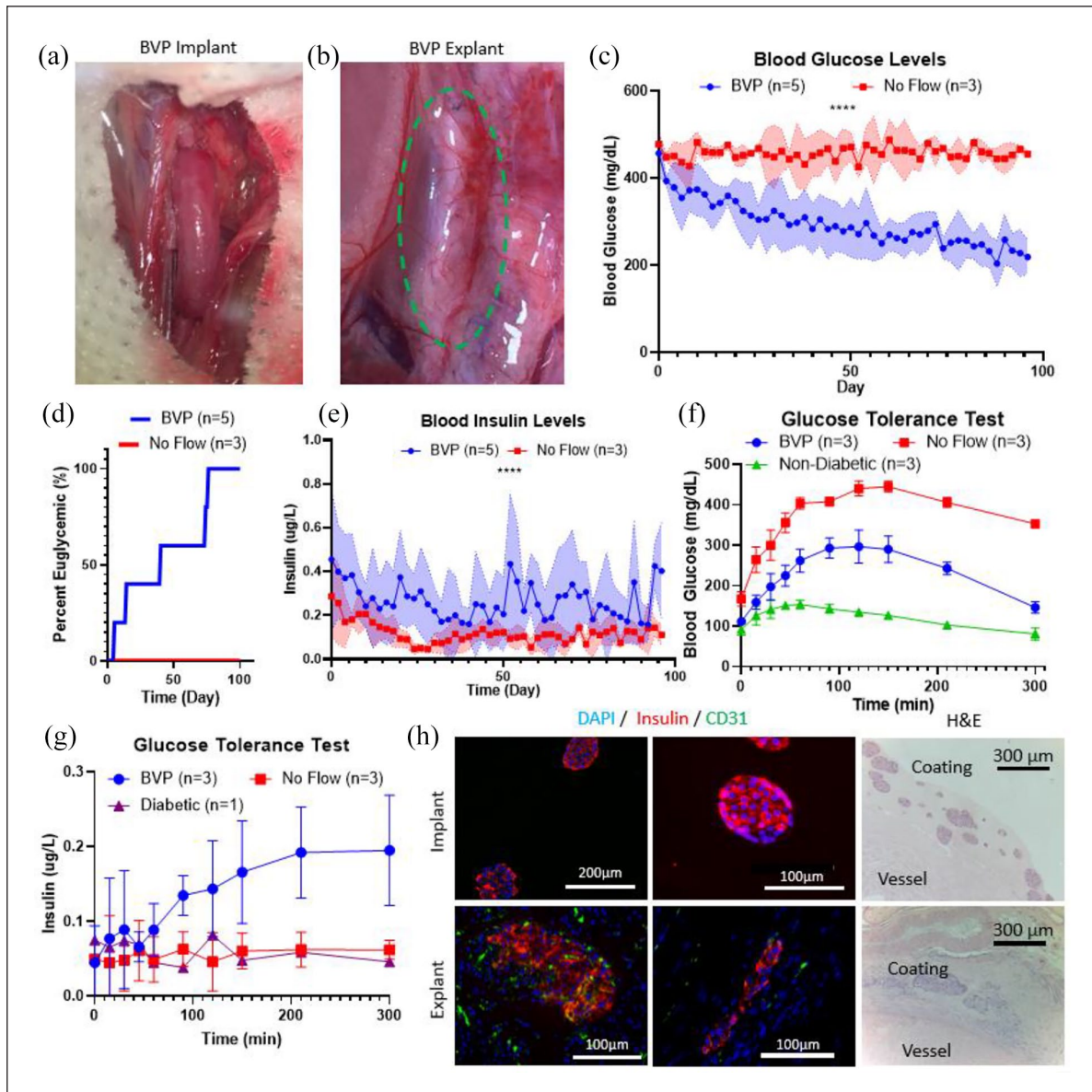


Figure 4. Demonstration of rat BVP therapeutic potential in streptozotocin induced diabetic nude rats. (a) BVP implanted into rat as an end-to-end abdominal aorta graft. (b) After 3 months, the BVP (green dotted circle) demonstrates robust microvascularization on the surface. (c) Blood glucose curves demonstrating restoration of euglycemia from BVP implants anastomosed as end-to-end grafts, no flow implants did not restore euglycemia. Statistical analysis was performed using a t-test analyzing mean values for each group ($****p < 0.0001$). (d) Survival plot demonstrating percent euglycemic (two consecutive blood glucose measurements < 250 mg/dL) rats. (e) Blood plasma insulin levels for rats after transplantation. Statistical analysis was performed using a t-test with mean values ($****p < 0.0001$). (f) Blood glucose levels and (g) insulin levels for intraperitoneal glucose tolerance test performed on day 90+ after implantation. (h) Staining for BVPs before implantation and after explantation demonstrating islet survival in the BVP. Islets are still found in vicinity of vessel outer surface after explantation.

abdominal aorta prevented this conventional graft removal approach. Instead, analysis of rat pancreata after BVP harvests were performed (Supplemental Figure 7). Staining results showed that there were no insulin positive cells in these pancreata, which demonstrates that the reduction of blood glucose and increase in insulin were due to the BVP graft as opposed to endogenous recovery from streptozotocin.

Glucose tolerance tests were performed at 3 months to quantify transplant efficacy. Rats with aortic-implanted BVPs ($n = 3$), “no flow” BVP rats ($n = 3$), and non-diabetic healthy rats ($n = 3$) were injected with 2 g/kg glucose into the intraperitoneal space. Blood was then sampled from the tail vein at 15, 30, 45, 60, 90, 120, 150, 210, and 300 min. Rats that received an anastomosed BVP demonstrated graft functionality by restoring near-normoglycemia, while

glucose levels in no flow BVP rats remained elevated for the duration of the glucose challenge (Figure 4(f)) (Supplemental Figure 8). A rise in blood plasma insulin was also detected in the anastomosed BVP group, with an upward trend extending to 300 min post injection (Figure 4(g)). Similar insulin trends were not observed in “no flow” BVP rats. It is interesting that the rate at which blood glucose decreases was noticeably slower than the native non-diabetic control, implying that the number of viable islets in the small BVP implant may not have been sufficient to completely restore normal insulin reactivity. Slow transport of insulin through the BVP graft may be another potential reason for the delay in graft functionality.

Insulin staining on explant cross sections showed long term survival of implanted rat islets in the BVP for up to 3 months (Figure 4(h)). Microvascular infiltration (Figure 4(b)) was confirmed by CD31 staining for endothelial cells (Figure 4(h)), providing evidence that islets were able to integrate into the vascular system of the host. The occurrence of microvascularization may explain why the BVP gradually restored normoglycemia over the course of 2 months: insulin secretion from islets is limited when local oxygen concentrations are low,⁵⁸ but as microvessels grow into the BVP, islets may become vascularized and be exposed to higher oxygen levels, thereby improving their insulin reactivity. Taken together, these results demonstrate that the anastomosed BVP is capable of restoring normoglycemic conditions in nude rats with streptozotocin-induced diabetes phenotype.

In vivo pig studies

To determine whether larger-scale BVPs could be produced, implanted, and show evidence of function, large BVPs were produced for diabetic, immunosuppressed pigs. Yucatan miniature swine, weighing ~30 kg, were rendered diabetic by injections with streptozotocin. Porcine islets were harvested from freshly excised pancreata obtained from adult Yorkshire swine, and were suspended in fibrin gels and coated around the outside of tissue engineered human acellular blood vessels, 6 mm in diameter and 20 cm in length (Figure 5(a)). Porcine islet isolation procedures proved technically challenging, and only limited total numbers of islets were utilized in porcine BVPs. Fibrin coatings were approximately 400 μ m in thickness, and harbored roughly 10,000–25,000 porcine islets, whereas approximately 375,000 islets are required to restore normoglycemia in a 30 kg pig.⁷⁵

To quantify potential BVP performance and insulin production resulting from the limited islet complement of the porcine BVPs, 1-cm segments of the BVPs were sampled prior to implantation. Assessment of porcine BVP segments predicted that the entire BVP could secrete 0.36 U of insulin each day, but since swine typically requires 0.6–1 IU/kg of insulin each day, we did not expect complete reversal of the diabetic phenotype in these animals receiving BVP

implants.^{76,77} Nonetheless, we undertook the experiments to determine whether any physiological effects of the BVP could be measured, and whether islet viability could be maintained by the BVP in a large animal model.

Since the recipient Yucatan miniature swine were immunocompetent, immunosuppression using tacrolimus (ranging from 0.25 mg/kg twice daily to 0.75 mg/kg twice daily), mycophenolate mofetil at 20–40 mg/kg each day, and a single dose of solumedrol 250 mg IV was given on the day of BVP implantation. A total of three diabetic pigs received BVP implants. Doses of tacrolimus and mycophenolate mofetil were increased in the latter two pigs after an observation of sub-therapeutic tacrolimus levels in the first animal.

Two BVPs were implanted into the neck (as side-to-side arteriovenous grafts from the right common carotid artery to the left external jugular vein; first and third animals) (Figure 5(b)), while one BVP was implanted into the abdomen as an end-to-side arteriovenous graft from the iliac artery to the contralateral iliac vein. The abdominal implant displayed some decrease of blood glucose for one week after implantation (Figure 5(c)), but was complicated by intra-abdominal bacterial sepsis. The third animal received an implant in the neck, with a BVP containing 10,000 islets and this animal also had therapeutic serum levels of tacrolimus (trough tacrolimus level of 8.6 ng/mL). This third animal also showed a short-term decrease in blood glucose for several days (Figure 5(d)). Immunosuppression for this third animal was initiated 5 days prior to transplantation.

Glucose tolerance tests were performed in the third animal. Despite having a subtherapeutic number of islets, implanting the BVP caused a detectable therapeutic effect by lowering blood glucose levels for the glucose tolerance test to pre-immunosuppression levels (Figure 5(e)). (The glucose tolerance test after BVP implantation was compared to pre- (7 days prior to transplantation) and post- (2 days prior to transplantation) initiation of immunosuppression, since immunosuppression itself can affect blood glucose levels and insulin sensitivity^{78–80}). While the small number of islets delivered did not restore normoglycemia in these diabetic swine, there was a measurable decrease in blood glucose after implanting the BVP in the third animal, and 2/3 animals displayed decreases in blood glucose for several days after BVP implantation (Supplemental Figure 9).

Immunofluorescent staining of the BVP implant showed fragments of porcine islets (Figure 5(f)). Explantation of the porcine BVPs at 2 weeks show survival of these implanted islet fragments and persisting presence of insulin (Figure 5(f)) H&E results showed minimal to no fibrosis was detected on the explant surface, indicating lack of fibrotic encasement that could limit nutrient transfer (Figure 5(g)). The H&E staining showed some fibrin on the outer surface of the acellular vessel with cells that match the size of the implanted islet fragments. While the fibrin coating was initially intended (via

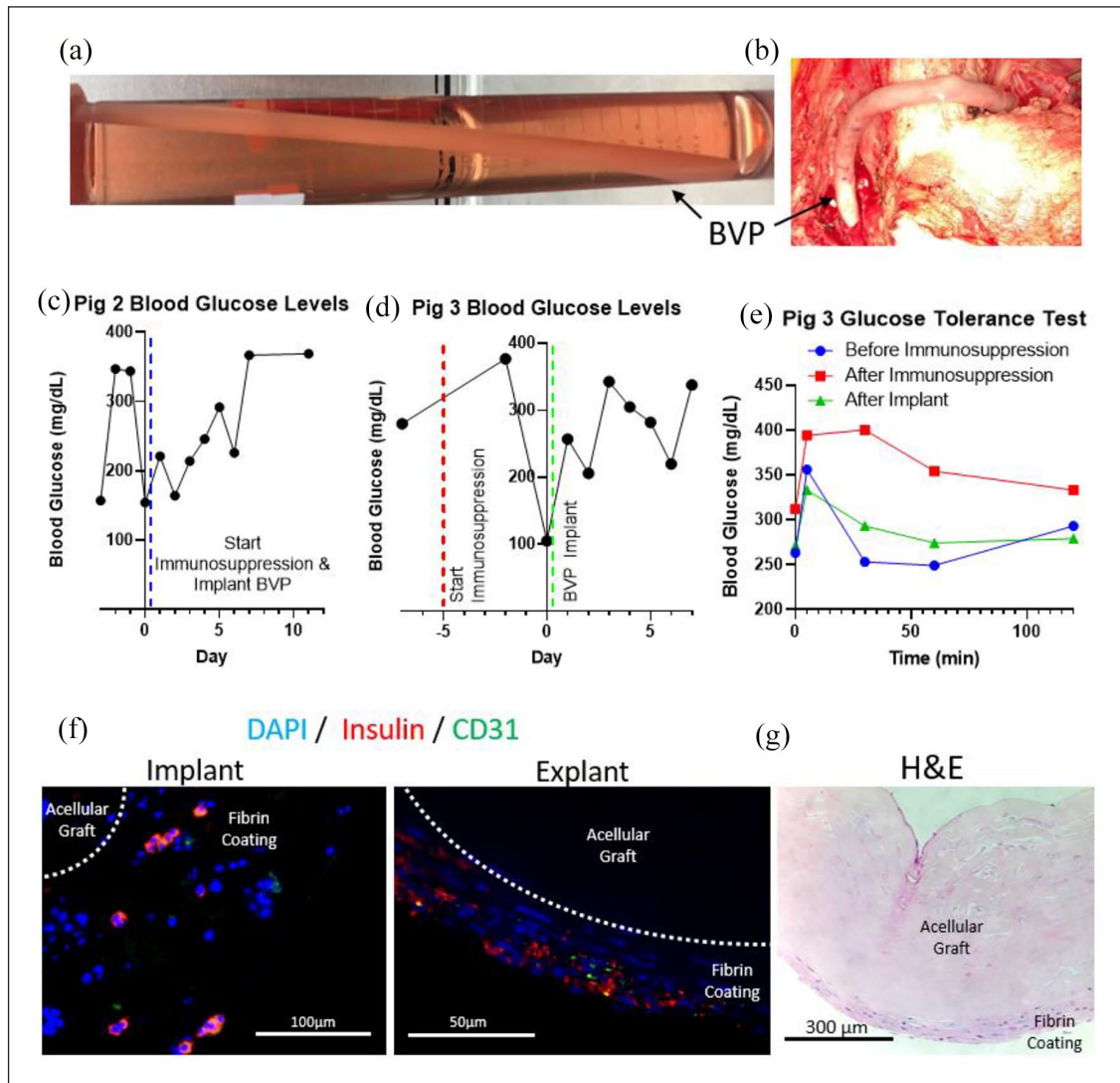


Figure 5. Scaled-up BVP implantations into immunosuppressed, streptozotocin induced diabetic pigs: (a) BVP 20 cm in length with an inner diameter of 6 mm and outer diameter of 8 mm, (b) BVP implanted as a side-to-side arteriovenous graft from the right common carotid artery to the left external jugular vein, (c) blood glucose levels for second pig that received a BVP implant, (d) blood glucose levels and (e) glucose tolerance test for third pig that received a BVP implant, (f) implant with pancreatic islet fragments containing beta cells in the implant (left) and explant (right), and (g) H&E image of explanted BVP demonstrating no fibrosis on the BVP surface.

molding dimensions) to be 400 μm , Figure 5(f) and (g) show fibrin layers thinner than 400 μm .

Discussion/Conclusion

Though many variations of techniques for islet transplantation exist, few are able to support islets through the initial avascular period after islet transplant to enable long term graft functionality in a clinical setting. The Edmonton Protocol is currently the only clinically approved method for islet transplantation. However, only 25%–50% of all islet transplantation recipients remain insulin-independent after 5 years, due in part to the detrimental effects of hypoxia on transplanted islet survival.^{22,23} In addition, due

to significant islet loss after transplantation, many islet transplantation procedures require multiple donor organs to produce sufficient islets for a single patient (2–12 donors)^{24–26} which places a significant strain on the donor pool. Considerable improvements in islet survivability during and after transplantation are required before the Edmonton Protocol can become a widely accepted treatment for T1D.²²

Immunoisolation technologies such as alginate microcapsules, or macrocapsule devices such as the Viacyte and Theracyte implants, have shown promise in rodent studies but fail to perform when scaling up to clinically relevant sizes for human patients.^{81–83} In addition, the majority of these technologies are transplanted into the subcutaneous

or intraperitoneal spaces which only have local oxygen levels around 40 mmHg O_2 . Low device surface area, sub-optimal local oxygen tensions, and a lack of vascularization adjacent to islets eventually lead to deficiencies in oxygen and nutrient transfer and islet graft failure.⁹

Other technologies aim to directly aid in islet survival by increasing local oxygen availability for transplanted islets. The beta air device houses microencapsulated islets connected to an external subcutaneous oxygen port. By injecting oxygen into the port, islets are directly supplied with oxygen to decrease the risk of hypoxia.^{84,85} Though promising results have been achieved in pre-clinical studies, the burden of patient compliance is shifted from blood glucose monitoring/insulin injections toward daily injections of oxygen into the beta air's oxygen port.³⁴ Post-transplant administration of hyperoxic inhaled air has also been tested to improve islet transplant survival. Results indicated that supplying rats with 50% oxygen increased interstitial oxygen tension from 40 to 140 mmHg O_2 and improved survivability for islets implanted in the subcutaneous space. A major downside to this method is oxygen toxicity, which can occur when inhaling oxygen at a concentration only slightly greater than that of normal air.^{86,87} Other technologies aim to seed islets with oxygen-generating scaffolds to improve oxygen availability immediately post-transplantation.^{35,88} Development of these types of techniques to improve oxygen availability highlights the need to prevent hypoxia in transplanted islets.

Transplantation into highly vascularized areas of the body represents another way to increase oxygen availability to improve islet survival. For example, sites such as the kidney capsule and omentum are being investigated for islet transplantation.⁸⁹⁻⁹¹ While transplanting islets into these sites has been shown to quickly reverse diabetes in animal models, using these sites may not be clinically practical in human patients, due to the invasiveness of the procedure and difficulty of graft removal.

Engineering a new vascular site for islet transplantation is a less explored approach but may offer the greatest benefits for islet transplantation. One group is pursuing repopulation of decellularized rat pancreata with islets to create an artificial pancreas.⁹² Though this strategy reintroduces islets to their native niche, the majority of a pancreas is comprised of exocrine ECM rather than endocrine ECM. Another approach is to seed islets into the trachea of a decellularized lung.⁷⁰ Results from this approach showed increased survival of islets thanks to the high density of microvessels present in alveoli. Both these approaches require anastomosis to the patient for full vascular integration, however, and can be limited by thrombosis of microvessel structures within the decellularized organ. Encouraging vessel ingrowth using prevascularization or angiogenic factors can also be used to further encourage vascular integration of islets with the patient.^{52,93}

The BVP utilizes a large diameter vascular graft with a diameter of 6 mm to support blood flow to transplanted islets. Grafts of this size are far less prone to thrombosis due to laminar flow and high flow rates.⁴⁷ Islets seeded on the BVP are in close proximity to blood flow but do not directly contact blood, which mitigates the risk for instant blood mediated inflammatory reactions against the islets. Surgically, BVPs may be implanted as an arterial or an arteriovenous graft in the arm: arteriovenous grafting is typically a simple outpatient procedure. Previous trials using tissue engineered large diameter grafts utilized 75–325 mg of orally administered aspirin per day for anticoagulation.⁴⁷ Blood flow rates through an arteriovenous graft are typically on the order of 1 liter/minute, providing abundant oxygen delivery to islet situated just outside the graft wall.⁴⁷ As such, the BVP design represents a safe and effective vascular technique for islet transplantation.

The BVP is also capable of extensive remodeling due to the biocompatible components used in its construction. Cellular infiltration with the graft may impact O_2 kinetics but this may be offset by the gradual integration of islets with the host's microvascular system.

To help to overcome the challenges of delivering a sufficient number of islets to treat humans, the BVP maintains a consistent volume to surface area ratio for a monolayer of islets disposed on the outer surface of an acellular arterial or arteriovenous conduit (Supplemental Table 1). We selected fibrin as the coating hydrogel since it is naturally involved in the wound healing and revascularization process. As a tradeoff, however, this means that BVP implants do not directly incorporate immune-isolation. Thus, BVP graft recipients are required to take immunosuppressants,^{94,95} which would be a tradeoff for the deleterious effects uncontrolled type 1 diabetes. Future work on the BVP may aim to integrate new technologies being developed such as conformational islet coating or immune-privileged beta cells that are derived from human embryonic stem (ES) or induced pluripotent stem (iPS) cells, that may limit the need for immune suppression for BVPs in the future.⁹⁶⁻⁹⁸

Taken together, this work represents an intersection of in silico modeling, in vitro bioreactor testing, and in vivo tissue implantation studies to evaluate the efficacy of a potentially improved islet transplantation therapy.

Materials and methods

In silico modeling in COMSOL multiphysics

Finite element analysis modeling was performed in COMSOL Multiphysics® (Version 5.4-5.5) (Burlington, MA). The Transport of Diluted Species Module was used to simulate islet behavior and diffusion with respect to oxygen consumption. The module was governed by Fick's First Law ($J_{O_2} = D_{O_2} \nabla C_{O_2}$), where J_{O_2} is the molar flux of

oxygen [$\text{mol}/(\text{m}^2\text{s})$], D_{O_2} is the diffusion coefficient of oxygen [m^2/s] and C_{O_2} is oxygen concentration [mol/m^3]. Parameters used for islet modeling were obtained from previous work done by Buchwald et al.^{58–60} For Buchwald's studies, islet oxygen consumption was simulated using a Michaelis-Menten equation [$R = -R_{\text{max}} (C_{\text{O}_2}/C_{\text{O}_2} + K_m)$] where R_{max} is the maximal O_2 consumption rate per unit volume [$\text{mol}/(\text{m}^3\text{s})$], C_{O_2} is the concentration of oxygen [mol/m^3], and K_m is the half maximal concentration [mol/m^3]. He parameterized the equation to fit in vitro data collected using high resolution quantitative monitoring of islet secretion over time and the oxygen consumption of islets (R_{max}) was determined to be $0.034 \text{ mol O}_2/\text{s}/\text{m}^3$ while the half-maximal concentration (K_m) was $0.001 \text{ mol}/\text{m}^3$. Diffusion coefficients for islets were utilized as previously reported (for oxygen. Diffusion coefficients of oxygen for islets ($2.0 \times 10^{-9} \text{ m}^2/\text{s}$) decellularized vessels ($1.25 \times 10^{-9} \text{ m}^2/\text{s}$), fibrin ($1.7 \times 10^{-9} \text{ m}^2/\text{s}$), and culture media ($2.86 \times 10^{-9} \text{ m}^2/\text{s}$) were obtained from literature.^{99,100}

Geometrical representations of a BVP cross section including the lumen, decellularized vessel, and hydrogel coating were generated to simulate the BVP construct in silico. To create an accurate geometrical representation of islets the BVP, islet diameters were stochastically assigned utilizing a Weibull Distribution to replicate real world variations in islet diameter. In addition, islets were randomly distributed throughout the hydrogel layer to replicate the randomness of islet positions in the hydrogel layer of real BVP constructs. Running the COMSOL simulation with these properties allowed for stochastic simulations to account for the potential variations in islet diameter and position in the BVP.

To determine islet survival of the BVP construct, stationary solver studies were performed to determine the steady state oxygen levels experienced by islets in the BVP. Boundary conditions were assigned to mimic the conditions of the BVP in vivo – to replicate fully oxygenated arterial blood, the pO_2 of the vessel lumen was set to 100 mmHg O_2 ($1.4 \text{ mol}/\text{m}^3$) while the interstitial space outside the hydrogel coating was set to 40 mmHg O_2 ($0.5 \text{ mol}/\text{m}^3$).^{101–103} With regard to the lumen PO_2 level, since blood flow can be $>1 \text{ L}/\text{min}$ in the lumen of arteriovenous fistulas, longitudinal location of the cross section was determined to not be a rate limiting factor affecting oxygen concentration in the lumen. In silico islet survival was then quantified by calculating the surface integral of the simulated islets and determining the percent area below a critical oxygen threshold of 0.071 mmHg ($0.1 \mu\text{M}$) O_2 or functional threshold of 2 mmHg ($3 \mu\text{M}$) O_2 .^{58–60}

Acellular grafts. Umbilical cords categorized as discarded tissues were acquired from Yale New Haven Hospital through the Vascular Biology and Therapeutics Program at Yale School of Medicine. Following procurement, umbilical arteries were separated from the umbilical cord using

forceps to tear away the Wharton's jelly and artery adventitia. The isolated artery lumens were then flushed with phosphate-buffered saline (PBS) to remove any residual blood. Decellularization was performed as previously described.¹⁰⁴ Briefly, arteries were placed in CHAPS buffer (1 M NaCl, 25 mM EDTA, 8 mM CHAPS, PBS) and rocked overnight. Following PBS rinsing, the arteries were then placed in sodium dodecyl sulfate (SDS) buffer (1 mM NaCl, 25 mM EDTA, 1.8 mM CHAPS, PBS) and rocked overnight at 37°C . Extensive PBS washes were used to remove all residual detergents from the arteries. The vessels were then incubated in 10% fetal bovine serum (FBS)/1% Penicillin-Streptomycin (P/S) at 37°C for 48 h to remove residual DNA. Finally, the decellularized vessels were stored at 4°C in sterile PBS with 1% P/S solution. Decellularized umbilical arteries were used for all in vitro and rat implantation experiments.

For pig studies, Humacyte[®] (Durham, NC) acellular vessels were obtained directly from Humacyte[®] and stored at 4°C in sterile PBS with 1% P/S. Humacyte vessels are manufactured by culturing human smooth muscle cells (SMCs) on polyglycolic acid (PGA) tubular scaffolds in state-of-the-art bioreactors. During bioreactor culture, SMCs deposit extracellular matrix while the PGA degrades. The resultant vessel is then decellularized and made ready for use.

Animals. Sprague Dawley rats (3–6 months old; 250–400 g) served as islet donors for rat islet in vitro experiments and implantation studies. Male nude rats between 50 and 56 days old (200–300 g) were purchased from Charles River Labs (Wilmington, MA) served as transplant recipients. Yorkshire pigs (150–250 kg) were obtained from Oak Hill Genetics (Ewing, IL) and were used as pancreatic islet donors. Sinclair Bioresources (Auxvasse, MO) provided streptozotocin induced diabetic Yucatan pigs (25–30 kg) to serve as BVP recipients. All pigs were housed at Synchrony Labs (Durham, NC). All pig husbandry was managed by Synchrony Labs in accordance to The Guide for the Care and Use of Laboratory Animals. Protocols involving rats were approved by Yale Institutional Animal Care and Use Committee (IACUC) while protocols involving pigs were approved by Synchrony IACUC. All animal work complied with the NIH Guide for the Care and Use of Laboratory Animals.

Rat islet isolation and culture. Protocol for islet isolation was performed based on a previously published method.^{105,106} Sprague Dawley rats were euthanized using ketamine/xylazine. After the pancreas was separated from the surrounding tissue, it was cut into pieces $<0.5 \text{ cm}$ to better facilitate collagenase digestion and was placed into a vial containing 10 mL of $1.5 \text{ mg}/\text{mL}$ collagenase P ($2.1 \text{ U}/\text{mg}$) with HBSS (HBSS, 1% P/S, 3.25% HEPES). The vial was then agitated at 200 RPM at 37°C for 18–20 min.

The resultant solution was then filtered through a 500 μm nylon mesh and the solution was centrifuged at 1000 RPM for 1 min. Washes with HBSS were performed. Following the final wash, the pellet was resuspended in histopaque 1077 (Sigma-Aldrich; Cat. #10771) and a layer of basal RPMI 1640 (ThermoFisher Cat. #72400120) was carefully added on top of the histopaque solution. Centrifugation at 2500 RPM for 20 min at 4°C was used to purify islets away from exocrine cells/tissue. Islets purified into the boundary between the histopaque and RPMI were carefully extracted and placed into a separate centrifuge tube. Islets were then cultured with RPMI media with 10% FBS and 1% P/S at 50 islets/mL in suspension culture petri dishes. Culture media was changed once every 2 days.

Live/Dead characterization. To determine survival in various conditions, rat islets and rat BVP constructs were characterized using fluorescein diacetate (FDA) (Sigma-Aldrich; Cat. #F7378)/propidium iodide (PI) (Sigma-Aldrich; Cat. #4170). Tissues were incubated in 0.25 μM FDA 15.7 μM PI for 5 min at 37°C. Images were taken using a Lecia DMI6000B microscope and images were processed in ImageJ.

Fibrin hydrogel studies. Fibrin was created by mixing bovine fibrinogen (Sigma-Aldrich; Cat. #F8630) with thrombin (Sigma-Aldrich; Cat. # T4648) at a 100 mg:1 U ratio. (Bovine fibrinogen and thrombin were used to avoid the prohibitive cost of utilizing rat fibrinogen). Fibrinogen was prepared at varying concentrations in basal (serum free) RPMI media while thrombin was prepared at 2 U/mL in 0.1%BSA (Sigma-Aldrich; Cat. #A9418) in PBS. 10 mM CaCl_2 (Sigma-Aldrich; Cat. #449709) was added to fibrinogen to facilitate fibrin crosslinking while tranexamic acid (Cayman Chemical; Item #19193) was added at 160 $\mu\text{g}/\text{mL}$ to prevent fibrin degradation. Testing survival of islets in fibrin was performed by suspending 500 islets in 300 μL of fibrin in 24 well plates. After allowing the fibrin 20 min to polymerize, 500 μL of full RPMI media was added above the fibrin gel. Media was changed at day 2 and live/dead staining with FDA/PI was performed at day 1 and 3 to assess viability.

BVP creation process. BVPs were created using a combination of an acellular graft, fibrin hydrogel, and pancreatic islets. To start, bovine fibrinogen was prepared at 10 mg/mL in basal RPMI media with CaCl_2 and tranexamic acid as described above. To create rat sized BVPs, a 14-gauge blunt metal syringe was cannulated through the lumen of a decellularized human umbilical artery. A cylindrical polypropylene mold (inner diameter: 2 mm) was then coated with 5% pluronic F-127 (Sigma-Aldrich; Cat. # P2443) to prevent the fibrin hydrogel from sticking to the mold. A pellet of ~1500 IEQs was then resuspended in fibrinogen and thrombin. The resultant mixture was then

pipetted into the mold and the decellularized vessel on the metal syringe was then quickly added into the center of the mold and gently agitated in order to evenly distribute throughout the coating. Following 5 min of agitation, the mold was then placed into a 37°C incubator for 15 min to allow for the fibrin to fully polymerize. The mold was intermittently rotated during the incubation period in order to prevent islets from unevenly settling during the polymerization process. After the fibrin polymerized, the mandrel is gently removed from the mold. Since the mold was previously coated with pluronic F-127, the fibrin stuck solely onto the decellularized vessel and was successfully coated on the outer surface of the decellularized vessel. The BVP was then carefully pushed off the metal syringe using tweezers and kept in full RPMI media before being used for in vitro testing or in vivo implantation.

For pig sized BVPs, a Humacyte® human acellular vessel (HAV) was used as the primary scaffold for the BVP. A custom sized glass tube with 8 mm inner diameter created by Yale's Scientific Glassblowing Laboratory was used for the mold and a 6.0 mm OD metal mandrel was used to hold the HAV. A similar procedure to the rat BVP was then followed in order to coat the acellular vessel with fibrin and islets. One notable difference was that the HAV surface was smoother than umbilical artery surface which sometimes resulted in the fibrin coating slipping off of the HAV. To counteract this, the HAV was incubated in 50 $\mu\text{g}/\text{mL}$ fibronectin for 30 min prior to the coating protocol to ensure coating integrity.

In vitro BVP testing. Insulin secretion capabilities of the BVP were assessed using a static incubation experiment. Following the creation of the BVP, it was then incubated (37°C, 20% O_2 , 5% CO_2) in glucose free media (<20 mg/dL glucose) for 60 min and then switched to glucose media (180 mg/dL glucose) for 120 min. Media was sampled every 15 min and samples were assessed using a High Range Rat Insulin ELISA kit (Mercodia; Cat. # 10-1145-01).

Survival studies were performed to compare the BVP in static incubation settings versus bioreactor settings. For static incubation, BVPs were created and left either in a normal incubator (160 mmHg O_2) or a hypoxia chamber (40 mmHg O_2) in a 100 mm \times 20 mm petri dish with 20 mL of media to fully submerge the BVP. For bioreactors, the BVP was carefully cannulated into a bioreactor with separate lumen and interstitial reservoirs. The interstitial reservoir surrounds the BVP and a hypoxic oxygen mixture (5% O_2) is used to keep the interstitial reservoir media at a pO_2 of ~40 mmHg. The lumen reservoir was attached to a pump that pumps media through the lumen of the BVP and was attached to a 100 mmHg oxygen tank (12.5% O_2). Both static incubations and bioreactors were run for 2 days. Results were analyzed using both FDA/PI staining and histology.

Implantation in diabetic rats. Streptozotocin injections (65 mg/kg in 50 mM sodium citrate, I.P.) (Sigma-Aldrich; Cat. #S0130) were used to induce diabetes in graft recipient nude rats as previously described.¹⁰⁷ Animals with two consecutive non-fasting glucose measurements above 400 mg/dL were considered diabetic and qualified for surgery. Rats that did not meet this requirement received a repeat streptozotocin injection.

To test functionality *in vivo*, BVPs were implanted as end-to-end abdominal aorta interposition grafts into diabetic nude rats similar to previously performed protocols.¹⁰⁸ Rats were anesthetized with isoflurane and injected with buprenorphine and bupivacaine for analgesia. After shaving and sterilizing the skin, a midline incision was made in the abdomen and the intestines were retracted outwards and wrapped in saline-moistened gauze. The infra-renal abdominal aorta was then carefully separated from the surrounding tissue. Two microvascular clamps were placed on the abdominal aorta for vascular control and a transection was made between the two clamps. The BVP was then placed at the transection site and an interposition graft was constructed. Anastomoses were created using 10-0 monofilament nylon suture (AROSuture; Cat# T04A10N07-13). Clamps were then removed to allow for blood flow through the graft. The intestines were then returned to the abdominal cavity and the abdomen was sutured closed. Post-surgery, rats were administered meloxicam or ketoprofen for analgesia every 24 h for 48 h and were housed in individual cages.

Monitoring rats – blood glucose sampling, glucose tolerance test. Blood samples were obtained using a tail nick procedure. Blood was collected into a heparinized tube and centrifuged at 5000 RCF for 10 min. The plasma supernatant was collected and used for testing in a glucometer (Gluc-Cell®, CESCO Bioengineering, Trevose, PA). The remaining plasma was frozen at -20°C until being used for ELISA insulin testing (Mercodia, Sweden).

Glucose tolerance tests (GTT) were performed. Rats were fasted overnight and a baseline blood sample was acquired at noon. Rats were then injected with 2 g/kg glucose in physiological saline into the intraperitoneal space. Blood was then sampled at 15, 30, 45, 60, 90, 120, 150, 210, and 300 min.

Porcine islet isolation and porcine BVP implantation. Porcine islet isolation was performed based on a previously published protocol with modifications.¹⁰⁹ Briefly, porcine pancreata were acquired and placed in Wisconsin buffer solution for transport. The common bile duct was then cannulated and inflated with 1.5 U/mL collagenase at 2 mL per gram of pancreas weight. Pancreata were then digested with agitation for 5 min and solution was quenched with an equivalent volume of ice cold HBSS with 10% FBS. Following multiple washes with centrifugation and removal of supernatant,

the pancreas tissue was resuspended in histopaque 1077 and layered with a gradient of basal RPMI. Centrifugation for 20 min was then used to separate islets from exocrine tissue. Porcine islet isolations were performed 1–2 days prior to porcine BVP implantation.

An intravenous glucose tolerance test was performed on Yucatan streptozotocin induced diabetic pigs slated for BVP implantation 7 days prior to implantation. Starting 5 days prior to the implantation process, pigs were provided with daily tacrolimus (0.75 mg/kg twice daily) and MMF (40 mg/kg twice daily) orally for immunosuppression. A glucose tolerance test was also performed 4 days prior to surgery. 3 days prior to surgery, Plavix (1 mg/kg) was provided orally as an anti-platelet therapy. 24 h prior to surgery, Fentanyl (50–100 mcg/h) was administered transcutaneously as an analgesia.

On the day of surgery, 250 mg of solumedrol was injected intravenously for immunosuppression. Porcine BVPs were constructed as previously described on the day of surgery. Anesthesia was induced using one dose of Ketamine (2.2 mg/kg), Telazol (4.4 mg/kg), Xylazine (2.2 mg/kg), and Marcaine (2–3 mg/kg) intramuscularly along with continuous Isoflurane (1%–4%) inhalation. Buprenorphine (0.01–0.05 mg/kg) was also injected intramuscularly as an analgesia during induction. During the surgery, Bretyllium (3–5 mg/kg) was administered intravenously every 30 min and Paralube was applied as needed onto the pig's eyes. Assessment of anesthesia through respiratory rate, heart rate, mucous membrane color, temperature, EKG, oxygen saturation, and reflexes was recorded every 15 min intraoperatively.

For implantation of the BVP into the neck, a midline neck incision was made and the carotid artery was exposed. Prior to vascular surgery, systemic heparinization (100 units/kg) was provided through the intravenous line and allowed to circulate for 3 min. The BVP was then anastomosed from the right common carotid artery to the left external jugular vein as a side-to-side implantation. One BVP implantation into the abdomen was also performed. For this surgery, a midline laparotomy was performed and the iliac artery was exposed. The BVP was then grafted from the iliac artery to the iliac vein as a side-to-side anastomosis.) After completion of the anastomoses and confirmation of blood flow through the BVP, the region was then sutured closed. For anti-platelet therapy, Aspirin (3–5 mg/kg) and Plavix (1 mg/kg) were provided orally every day after surgery. Tacrolimus and MMF continued to be provided at the previously mentioned dose and frequency. Post-operative analgesia was provided through Buprenorphine (0.01–0.05 mg/kg) intramuscularly every 12 h as needed for up to 7 days and Carprofen (4–5 mg/kg) intramuscularly every 24 h for up to 7 days.

Blood was collected daily from via IV blood draw or jugular vein catheter. A glucose tolerance test was performed 7 days after implantation. Blood glucose was

tested using a glucometer and porcine insulin was tested using Porcine Insulin ELISA kits (Merckodia; Cat. # 10-1200-01). Graft explantation was performed 2–4 weeks after implantation. After inducing anesthesia, heparin (200 units/kg) was injected to prevent coagulation, and a lethal injection of euthasol was provided.

Histology and immunostaining. BVPs were fixed in 10% neutral-buffered formalin overnight. Samples were embedded in paraffin, sectioned, and stained for H&E. Immunofluorescent staining was used to stain for insulin, HIF1- α , CD31, and CD45. To perform immunofluorescent staining, slides were rehydrated by baking at 65°C and performing sequential washes in xylene, 100%, 95%, 85%, 75%, and 50% EtOH. For antigen retrieval, slides were incubated with sodium citrate buffer at 70°C. Following a PBS wash, tissues were circled using a hydrophobic marker and blocking buffer was applied for 1 h. The slides were then incubated with the relevant primary antibody overnight (insulin – 1:200 (Abcam Cat. # ab7842); CD31 – 1:300 (Abcam Cat. # ab28364); HIF1- α – 1:100 (Abcam Cat. # ab1)). Six washes were then performed with 1% Triton PBS before incubating the slides with secondary for 1 h (Anti-GP – 1:500 (Abcam Cat. # ab150185); Anti-Rb – 1:500 (Abcam Cat. # 96919); Anti-Ms – 1:500 (Abcam Cat. # ab150113)). Slides were then washed four additional times and DAPI was applied to the slide with a coverslip on top. Fluorescent images were taken using a Lecia DMI6000B microscope. Images were processed using Lecia LAS AF and Image J.

Statistics. All data points and error bars represent mean \pm SD. Statistical analysis was performed in GraphPad Prism 8. Data were analyzed for statistical significance using unpaired two-tailed Student's *T*-test. Specific *P* values are included in figure captions.

Acknowledgements

The authors acknowledge Rebecca Cardone and Xiaojian Zhao for technical advice. We also acknowledge the IOMIC (Islet, Oxygen Consumption, Mass Isotopomer flux Core) facility as part of the Cell Bio core of the Yale Diabetes Research Center which assisted with living islet and rodent work. Finally, we thank George A Truskey for usage of his lab space at Duke University.

Data availability

The raw/processed data required to reproduce these findings cannot be shared at this time due to technical or time limitations.

Declaration of conflicting interests

The author(s) declared the following potential conflicts of interest with respect to the research, authorship, and/or publication of this article: L.E.N. is a founder and shareholder in Humacyte, Inc., which is a regenerative medicine company. J.H.L. is a shareholder in Humacyte Inc. Humacyte produces engineered blood vessels

from allogeneic smooth muscle cells for vascular surgery. L.E.N.'s spouse has equity in Humacyte, and L.E.N. and J.H.L. serve on Humacyte's Board of Directors. L.E.N. and J.H.L. are inventors on patents that are licensed to Humacyte and that produce royalties for L.E.N. and J.H.L. L.E.N. has received an unrestricted research gift to support research in her laboratory at Yale. Humacyte did not influence the description or interpretation of the findings in this report. The other authors report no conflicts.

Funding

The author(s) disclosed receipt of the following financial support for the research, authorship, and/or publication of this article: This study was supported by Yale University, by NIH R01-HL148819, and by an unrestricted research gift from Humacyte Inc (both to L.E.N.).

ORCID iD

Edward X Han  <https://orcid.org/0000-0002-5989-1747>

Supplemental material

Supplemental material for this article is available online.

References

1. Yoon JW and Jun HS. Autoimmune destruction of pancreatic beta cells. *Am J Ther* 2005; 12: 580–591.
2. Narayan KM, Gregg EW, Fagot-Campagna A, et al. Diabetes—a common, growing, serious, costly, and potentially preventable public health problem. *Diabetes Res Clin Pract* 2000; 50(Suppl 2): S77–S84.
3. Grundy SM, Benjamin IJ, Burke GL, et al. Diabetes and cardiovascular disease: a statement for healthcare professionals from the American Heart Association. *Circulation* 1999; 100: 1134–1146.
4. Juster-Switlyk K and Smith AG. Updates in diabetic peripheral neuropathy. *F1000Res* 2016; 5: F1000 Faculty Rev-738.
5. Brennan DC, Kopetskie HA, Sayre PH, et al. Long-term follow-up of the Edmonton protocol of islet transplantation in the United States. *Am J Transplant* 2016; 16: 509–517.
6. Olsson R, Olerud J, Pettersson U, et al. Increased numbers of low-oxygenated pancreatic islets after intraportal islet transplantation. *Diabetes* 2011; 60: 2350–2353.
7. Komatsu H, Cook C, Wang C-H, et al. Oxygen environment and islet size are the primary limiting factors of isolated pancreatic islet survival. *PLoS One* 2017; 12: e0183780.
8. Komatsu H, Kandeel F and Mullen Y. Impact of oxygen on pancreatic islet survival. *Pancreas* 2018; 47: 533–543.
9. Colton CK. Oxygen supply to encapsulated therapeutic cells. *Adv Drug Deliv Rev.* 2014; 67–68: 93–110.
10. de Groot M, Schuur TA, Keizer PPM, et al. Response of encapsulated rat pancreatic islets to hypoxia. *Cell Transplant* 2003; 12: 867–875.
11. Jansson L, Barbu A, Bodin B, et al. Pancreatic islet blood flow and its measurement. *Ups J Med Sci* 2016; 121: 81–95.
12. Jansson L and Hellerström C. Stimulation by glucose of the blood flow to the pancreatic islets of the rat. *Diabetologia* 1983; 25: 45–50.
13. Qi M, Lacik I, Kolláriková G, et al. A recommended laparoscopic procedure for implantation of microcapsules in the

- peritoneal cavity of non-human primates. *J Surg Res* 2011; 168: e117–e123.
14. Fotino N, Fotino C and Pileggi A. Re-engineering islet cell transplantation. *Pharmacol Res* 2015; 98: 76–85.
 15. Cao R, Avgoustiniatos E, Papas K, et al. Mathematical predictions of oxygen availability in micro- and macro-encapsulated human and porcine pancreatic islets. *J Biomed Mater Res Part B Appl Biomater* 2020; 108: 343–352.
 16. van der Windt DJ, Echeverri GJ, Ijzermans JN, et al. The choice of anatomical site for islet transplantation. *Cell Transplant* 2008; 17: 1005–1014.
 17. Naziruddin B, Iwahashi S, Kanak MA, et al. Evidence for instant blood-mediated inflammatory reaction in clinical autologous islet transplantation. *Am J Transplant* 2014; 14: 428–437.
 18. Suszynski TM, Avgoustiniatos ES and Papas KK. Oxygenation of the intraportally transplanted pancreatic islet. *J Diabetes Res* 2016; 2016: 7625947.
 19. Bennet W, Groth CG, Larsson R, et al. Isolated human islets trigger an instant blood mediated inflammatory reaction: implications for intraportal islet transplantation as a treatment for patients with type 1 diabetes. *Ups J Med Sci* 2000; 105: 125–133.
 20. Pepper AR, Gala-Lopez B, Ziff O, et al. Revascularization of transplanted pancreatic islets and role of the transplantation site. *Clin Dev Immunol* 2013; 2013: 352315.
 21. McCall M and Shapiro AMJ. Update on islet transplantation. *Cold Spring Harb Perspect Med* 2012; 2: a007823.
 22. Jin S-M and Kim K-W. Is islet transplantation a realistic approach to curing diabetes? *Korean J Intern Med* 2017; 32: 62–66.
 23. Shapiro AMJ, Ricordi C, Hering BJ, et al. International trial of the Edmonton protocol for islet transplantation. *N Engl J Med* 2006; 355: 1318–1330.
 24. van Kampen CA, van de Linde P, Duinkerken G, et al. Alloreactivity against repeated HLA mismatches of sequential islet grafts transplanted in non-uremic type 1 diabetes patients. *Transplantation* 2005; 80: 118–126.
 25. Korsgren O, Lundgren T, Felldin M, et al. Optimising islet engraftment is critical for successful clinical islet transplantation. *Diabetologia* 2008; 51: 227–232.
 26. Shapiro AM, Lakey JR, Ryan EA, et al. Islet transplantation in seven patients with type 1 diabetes mellitus using a glucocorticoid-free immunosuppressive regimen. *N Engl J Med* 2000; 343: 230–238.
 27. Iacovacci V, Ricotti L, Mencias A, et al. The bioartificial pancreas (BAP): biological, chemical and engineering challenges. *Biochem Pharmacol* 2016; 100: 12–27.
 28. Opara EC, McQuilling JP and Farney AC. Microencapsulation of pancreatic islets for use in a bioartificial pancreas. *Methods Mol Biol* 2013; 1001: 261–266.
 29. Pareta R, McQuilling JP, Sittadjody S, et al. Long-term function of islets encapsulated in a redesigned alginate microcapsule construct in omentum pouches of immune-competent diabetic rats. *Pancreas* 2014; 43: 605–613.
 30. Vaithilingam V and Tuch BE. Islet transplantation and encapsulation: an update on recent developments. *Rev Diabet Stud* 2011; 8: 51–67.
 31. Siebers U, Horcher A, Bretzel RG, et al. Transplantation of free and microencapsulated islets in rats: evidence for the requirement of an increased islet mass for transplantation into the peritoneal site. *Int J Artif Organs* 1993; 16: 96–99.
 32. Schneider S, Feilen PJ, Brunnenmeier F, et al. Long-term graft function of adult rat and human islets encapsulated in novel alginate-based microcapsules after transplantation in immunocompetent diabetic mice. *Diabetes* 2005; 54: 687.
 33. Bochenek MA, Veiseh O, Vegas AJ, et al. Alginate encapsulation as long-term immune protection of allogeneic pancreatic islet cells transplanted into the omental bursa of macaques. *Nat Biomed Eng* 2018; 2: 810–821.
 34. Carlsson P-O, Espes D, Sedigh A, et al. Transplantation of macroencapsulated human islets within the bioartificial pancreas β Air to patients with type 1 diabetes mellitus. *Am J Transplant* 2018; 18: 1735–1744.
 35. Lee EM, Jung JI, Alam Z, et al. Effect of an oxygen-generating scaffold on the viability and insulin secretion function of porcine neonatal pancreatic cell clusters. *Xenotransplantation* 2018; 25: e12378.
 36. Sullivan SJ, Maki T, Borland KM, et al. Biohybrid artificial pancreas: long-term implantation studies in diabetic, pancreatectomized dogs. *Science* 1991; 252: 718–721.
 37. Monaco AP, Maki T, Ozato H, et al. Transplantation of islet allografts and xenografts in totally pancreatectomized diabetic dogs using the hybrid artificial pancreas. *Ann Surg* 1991; 214: 339–362.
 38. Hou QP and Bae YH. Biohybrid artificial pancreas based on microcapsule device. *Adv Drug Deliv Rev* 1999; 35: 271–287.
 39. Pashneh-Tala S, MacNeil S and Claeysens F. The tissue-engineered vascular graft—past, present, and future. *Tissue Eng Part B Rev* 2016; 22: 68–100.
 40. Greenwald SE and Berry CL. Improving vascular grafts: the importance of mechanical and haemodynamic properties. *J Pathol* 2000; 190: 292–299.
 41. Radke D, Jia W, Sharma D, et al. Tissue engineering at the blood-contacting surface: a review of challenges and strategies in vascular graft development. *Adv Healthc Mater* 2018; 7: e1701461.
 42. Lin C-H, Hsia K, Ma H, et al. In vivo performance of decellularized vascular grafts: a review article. *Int J Mol Sci* 2018; 19: 2101.
 43. Tucker EI, Marzec UM, White TC, et al. Prevention of vascular graft occlusion and thrombus-associated thrombin generation by inhibition of factor XI. *Blood* 2009; 113: 936–944.
 44. Schaner PJ, Martin ND, Tulenko TN, et al. Decellularized vein as a potential scaffold for vascular tissue engineering. *J Vasc Surg* 2004; 40: 146–153.
 45. Kirkton RD, Santiago-Maysonet M, Lawson JH, et al. Bioengineered human acellular vessels recellularize and evolve into living blood vessels after human implantation. *Sci Transl Med* 2019; 11: eaau6934.
 46. Bibevski S, Ruzmetov M, Fortuna RS, et al. Performance of SynerGraft decellularized pulmonary allografts compared with standard cryopreserved allografts: results from multi-institutional data. *Ann Thorac Surg* 2017; 103: 869–874.
 47. Lawson JH, Glickman MH, Ilzecki M, et al. Bioengineered human acellular vessels for dialysis access in patients with end-stage renal disease: two phase 2 single-arm trials. *Lancet* 2016; 387: 2026–2034.

48. Paniccia A and Schulick RD. Chapter 4 - Pancreatic physiology and functional assessment. In: Jarnagin WR (ed.) *Blumgart's surgery of the liver, biliary tract and pancreas, 2-volume set* 6th ed. Philadelphia, PA: Content Repository Only!, 2017, pp.66–76.e3.
49. Seiron P, Wiberg A, Krogvold L, et al. Characterization of the endocrine pancreas in type 1 diabetes: islet size is maintained but islet number is markedly reduced. *J Pathol Clin Res* 2019; 5: 248–255.
50. Robertson RP, Lanz KJ, Sutherland DE, et al. Prevention of diabetes for up to 13 years by autoislet transplantation after pancreatectomy for chronic pancreatitis. *Diabetes* 2001; 50: 47–50.
51. Riopel M, Trinder M and Wang R. Fibrin, a scaffold material for islet transplantation and pancreatic endocrine tissue engineering. *Tissue Eng Part B Rev* 2014; 21: 34–44.
52. Najjar M, Manzoli V, Abreu M, et al. Fibrin gels engineered with pro-angiogenic growth factors promote engraftment of pancreatic islets in extrahepatic sites in mice. *Biotechnol Bioeng* 2015; 112: 1916–1926.
53. Riopel M, Li J, Trinder M, et al. Fibrin supports human fetal islet-epithelial cell differentiation via p70s6k and promotes vascular formation during transplantation. *Lab Invest* 2015; 95: 925–936.
54. Beattie GM, Montgomery AMP, Lopez AD, et al. A novel approach to increase human islet cell mass while preserving β -cell function. *Diabetes* 2002; 51: 3435–3439.
55. Kuehn C, Lakey JR, Lamb MW, et al. Young porcine endocrine pancreatic islets cultured in fibrin show improved resistance toward hydrogen peroxide. *Islets* 2013; 5: 207–215.
56. Sharony R, Keltz E, Biron-Shental T, et al. Morphometric characteristics of the umbilical cord and vessels in fetal growth restriction and pre-eclampsia. *Early Hum Dev* 2016; 92: 57–62.
57. Predanic M and Perni SC. Antenatal assessment of discordant umbilical arteries in singleton pregnancies. *Croat Med J* 2006; 47: 701–708.
58. Buchwald P. A local glucose-and oxygen concentration-based insulin secretion model for pancreatic islets. *Theor Biol Med Model* 2011; 8: 20.
59. Buchwald P, Cechin SR, Weaver JD, et al. Experimental evaluation and computational modeling of the effects of encapsulation on the time-profile of glucose-stimulated insulin release of pancreatic islets. *Biomed Eng Online* 2015; 14: 28.
60. Buchwald P, Tamayo-Garcia A, Manzoli V, et al. Glucose-stimulated insulin release: Parallel perfusion studies of free and hydrogel encapsulated human pancreatic islets. *Biotechnol Bioeng* 2018; 115: 232–245.
61. Buchwald P, Wang X, Khan A, et al. Quantitative assessment of islet cell products: estimating the accuracy of the existing protocol and accounting for islet size distribution. *Cell Transplant* 2009; 18: 1223–1235.
62. Johnson AS, Fisher RJ, Weir GC, et al. Oxygen consumption and diffusion in assemblages of respiring spheres: Performance enhancement of a bioartificial pancreas. *Chem Eng Sci* 2009; 64: 4470–4487.
63. Anundi I and de Groot H. Hypoxic liver cell death: critical P_{O_2} and dependence of viability on glycolysis. *Am J Physiol* 1989; 257: G58–G64.
64. Papas KK, Hering BJ, Guenther L, et al. Pancreas oxygenation is limited during preservation with the two-layer method. *Transplant Proc* 2005; 37: 3501–3504.
65. Avgoustiniatos ES and Colton CK. Effect of external oxygen mass transfer resistances on viability of immunoisolated tissuea. *Ann N Y Acad Sci* 1997; 831: 145–166.
66. Avgoustiniatos ES, Hering BJ, Rozak PR, et al. Commercially available gas-permeable cell culture bags may not prevent anoxia in cultured or shipped islets. *Transplant Proc* 2008; 40: 395–400.
67. Guven G, Hilty MP and Ince C. Microcirculation: physiology, pathophysiology, and clinical application. *Blood Purif* 2020; 49: 143–150.
68. Zhao H and Chappell JC. Microvascular bioengineering: a focus on pericytes. *J Biol Eng* 2019; 13: 26.
69. Allen P, Melero-Martin J and Bischoff J. Type I collagen, fibrin and PuraMatrix matrices provide permissive environments for human endothelial and mesenchymal progenitor cells to form neovascular networks. *J Tissue Eng Regen Med* 2011; 5: e74–e86.
70. Citro A, Moser PT, Dugnani E, et al. Biofabrication of a vascularized islet organ for type 1 diabetes. *Biomaterials* 2019; 199: 40–51.
71. Hara Y, Fujino M, Nakada K, et al. Influence of the numbers of islets on the models of rat syngeneic-islet and allogeneic-islet transplantations. *Transplant Proc* 2006; 38: 2726–2728.
72. Dimitrievska S, Wang J, Lin T, et al. Glycocalyx-like hydrogel coatings for small diameter vascular grafts. *Adv Funct Mater* 2020; 30: 1908963.
73. Schaschkow A, Mura C, Dal S, et al. Impact of the type of continuous insulin administration on metabolism in a diabetic rat model. *J Diabetes Res* 2016; 2016: 8310516.
74. Dong H, Altomonte J, Morral N, et al. Basal insulin gene expression significantly improves conventional insulin therapy in type 1 diabetic rats. *Diabetes* 2002; 51: 130.
75. Kin T, Korbitt GS, Kobayashi T, et al. Reversal of diabetes in pancreatectomized pigs after transplantation of neonatal porcine islets. *Diabetes* 2005; 54: 1032.
76. Hara H, Lin YJ, Zhu X, et al. Safe induction of diabetes by high-dose streptozotocin in pigs. *Pancreas* 2008; 36: 31–38.
77. Manell EAK, Rydén A, Hedenqvist P, et al. Insulin treatment of streptozotocin-induced diabetes re-establishes the patterns in carbohydrate, fat and amino acid metabolisms in growing pigs. *Lab Anim* 2014; 48: 261–269.
78. Jindal RM, Sidner RA and Milgrom ML. Post-transplant diabetes mellitus. The role of immunosuppression. *Drug Saf* 1997; 16: 242–257.
79. Penfornis A and Kury-Paulin S. Immunosuppressive drug-induced diabetes. *Diabetes Metab* 2006; 32: 539–546.
80. Li Z, Sun F, Zhang Y, et al. Tacrolimus induces insulin resistance and increases the glucose absorption in the jejunum: a potential mechanism of the diabetogenic effects. *PLoS One* 2015; 10: e0143405.
81. Agulnick AD, Ambruzs DM, Moorman MA, et al. Insulin-producing endocrine cells differentiated in vitro from human embryonic stem cells function in macroencapsulation devices in vivo. *Stem Cells Transl Med* 2015; 4: 1214–1222.
82. Boettler T, Schneider D, Cheng Y, et al. Pancreatic tissue transplanted in TheraCyte encapsulation devices is protected

- and prevents hyperglycemia in a mouse model of immune-mediated diabetes. *Cell Transplant* 2016; 25: 609–614.
83. Kumagai-Braesch M, Jacobson S, Mori H, et al. The TheraCyte™ device protects against islet allograft rejection in immunized hosts. *Cell Transplant* 2013; 22: 1137–1146.
 84. Barkai U, Rotem A and de Vos P. Survival of encapsulated islets: more than a membrane story. *World J Transplant* 2016; 6: 69–90.
 85. Ludwig B, Reichel A, Steffen A, et al. Transplantation of human islets without immunosuppression. *Proc Natl Acad Sci U S A* 2013; 110: 19054–19058.
 86. Haugaard N. Cellular mechanisms of oxygen toxicity. *Physiol Rev* 1968; 48: 311–373.
 87. Fridovich I. Oxygen toxicity: a radical explanation. *J Exp Biol* 1998; 201: 1203.
 88. Razavi M, Primavera R, Kevadiya BD, et al. A collagen based cryogel bioscaffold that generates oxygen for islet transplantation. *Adv Funct Mater* 2020; 30: 1902463.
 89. Berman DM, Molano RD, Fotino C, et al. Bioengineering the endocrine pancreas: intraomental islet transplantation within a biologic resorbable scaffold. *Diabetes* 2016; 65: 1350–1361.
 90. Szot GL, Koudria P and Bluestone JA. Transplantation of pancreatic islets into the kidney capsule of diabetic mice. *J Vis Exp* 2007; 9: 404.
 91. Stice MJ, Dunn TB, Bellin MD, et al. Omental pouch technique for combined site islet autotransplantation following total pancreatectomy. *Cell Transplant* 2018; 27: 1561–1518.
 92. Napierala H, Hillebrandt KH, Haep N, et al. Engineering an endocrine Neo-Pancreas by repopulation of a decellularized rat pancreas with islets of Langerhans. *Sci Rep* 2017; 7: 41777.
 93. Pepper AR, Gala-Lopez B, Pawlick R, et al. A prevascularized subcutaneous device-less site for islet and cellular transplantation. *Nat Biotechnol* 2015; 33: 518–523.
 94. Stucker F and Ackermann D. Immunosuppressive drugs - how they work, their side effects and interactions. *Ther Umsch*. 2011; 68: 679–686.
 95. Wijdicks EF. Neurotoxicity of immunosuppressive drugs. *Liver Transpl* 2001; 7: 937–942.
 96. Tomei AA, Manzoli V, Fraker CA, et al. Device design and materials optimization of conformal coating for islets of Langerhans. *Proc Natl Acad Sci U S A* 2014; 111: 10514.
 97. Kondo Y, Toyoda T, Inagaki N, et al. iPSC technology-based regenerative therapy for diabetes. *J Diabetes Investig* 2018; 9: 234–243.
 98. Yamaguchi T, Sato H, Kato-Itoh M, et al. Interspecies organogenesis generates autologous functional islets. *Nature* 2017; 542: 191–196.
 99. Ehsan SM and George SC. Nonsteady state oxygen transport in engineered tissue: implications for design. *Tissue Eng Part A* 2013; 19: 1433–1442.
 100. Al-Ani A, Toms D, Kondro D, et al. Oxygenation in cell culture: critical parameters for reproducibility are routinely not reported. *PLoS One* 2018; 13: e0204269.
 101. Tsai AG, Johnson PC and Intaglietta M. Oxygen gradients in the microcirculation. *Physiol Rev* 2003; 83: 933–963.
 102. Kumosa LS, Routh TL, Lin JT, et al. Permeability of subcutaneous tissues surrounding long-term implants to oxygen. *Biomaterials* 2014; 35: 8287–8296.
 103. Collins J-A, Rudenski A, Gibson J, et al. Relating oxygen partial pressure, saturation and content: the haemoglobin-oxygen dissociation curve. *Breathe (Sheff)* 2015; 11: 194–201.
 104. Gui L, Muto A, Chan SA, et al. Development of decellularized human umbilical arteries as small-diameter vascular grafts. *Tissue Eng Part A* 2009; 15: 2665–2676.
 105. Carter JD, Dula SB, Corbin KL, et al. A practical guide to rodent islet isolation and assessment. *Biol Proced Online* 2009; 11: 3–31.
 106. O'Dowd JF. The isolation and purification of rodent pancreatic islets of Langerhans. *Methods Mol Biol* 2009; 560: 37–42.
 107. Furman BL. Streptozotocin-induced diabetic models in mice and rats. *Curr Protoc Pharmacol* 2015; 70: 5.47.1–5.47.20.
 108. Gui L, Dash BC, Luo J, et al. Implantable tissue-engineered blood vessels from human induced pluripotent stem cells. *Biomaterials* 2016; 102: 120–129.
 109. Holdcraft RW, Green ML, Breite AG, et al. Optimizing porcine islet isolation to markedly reduce enzyme consumption without sacrificing islet yield or function. *Transplant Direct* 2016; 2: e86.